



# Vitrification of gamma irradiated $^{60}\text{Co}^{2+}$ zeolites

S. Bulbulian <sup>a,\*</sup>, P. Bosch <sup>b</sup>

<sup>a</sup> Instituto Nacional de Investigaciones Nucleares A.P. 18-1027. Col. Escandón, Delegación Miguel Hidalgo, C.P. 11801, México DF, Mexico

<sup>b</sup> Universidad Autónoma Metropolitana, Iztapalapa A.P. 55-532, Michoacán y La Purísima, Iztapalapa, C.P. 09340, México DF, Mexico

Received 31 May 2000; accepted 22 January 2001

## Abstract

A and X Co-exchanged zeolites were thermally treated until vitrification and, then, gamma irradiated. Desorption of cobalt from those treated solids was verified by ion exchange with 1N NaCl solution. As the calcining temperature increased, the crystallinity of cobalt exchanged zeolites decreased. At high temperatures (1000°C), the vitrification was an intermediate state as the amorphous compounds recrystallized in the form of nepheline. The irradiation induced small changes in the cell parameters. In X zeolite, irradiation treatment diminished the vitrification temperature. The vitrified samples, whether irradiated or not, safely trapped the cobalt originally present in the zeolites. The solids were characterized by X-ray diffraction, IR-spectroscopy and the cobalt content was determined by neutron activation analyses. © 2001 Elsevier Science B.V. All rights reserved.

## 1. Introduction

Treatment of hazardous wastes is an important topic, particularly when radioactivity is involved. Production of nuclear fuel and generation of nuclear energy is necessarily linked to the formation of a substantial amount of radioactive waste whose safe treatment and disposal are far from trivial. To limit potential human exposure and the leakage of dangerous material into the environment, nuclear wastewaters may be circulated through reactors containing ion exchanging materials, such as zeolites or clays. The sorption of  $\text{Co}^{2+}$  ions from aqueous solutions has been studied in our laboratory using NaX and NaA zeolites [1–3]. The exchanged aluminosilicate is, then, thermally treated to obtain a vitrified material that traps the radioactive elements. In this way, leaching to groundwater can be avoided. Moreover, the formation of glasses reduces the radioactive waste volume by 80% [4]. Still, the immobilization of radioisotopes in vitrified materials is a matter of controversy.

Under extreme conditions, the initially safe material could, indeed, present micropores and the radioactive ions could diffuse out. In this context the study by Földesová et al. [5] is most illustrative.  $^{137}\text{Cs}$  and  $^{60}\text{Co}$  were sorbed on chemically treated granular zeolite. The zeolite was, then, incorporated into cement slurries based on blast furnace slag, and leaching tests were performed in water, base and acid. Although no leaching out was observed in water or base solutions, contamination in acid solutions was found.

The use of vitrification in order to trap the radioactive isotopes in solids has been widely reported [6]. Glassy and amorphous materials are characterized by random, irregular structures, but even this group of materials possesses some structural layers [7,8] because of structural phase transitions. When they are subjected to a pressure and temperature treatment, an irreversible densification of vitreous silica can be achieved. This may be interpreted as a reconstructive transformation. Furthermore, glassy structures, if submitted to high doses of irradiation, may develop defects or recrystallize as a new phase. Devitrification behavior is not independent of treatments or composition. Marotta et al. [9] have shown that replacing PbO by  $\text{Li}_2\text{O}$  in a glass structure alters the glass transition temperature, which increases as  $\text{Pb}^{2+}$  ions are replaced by  $\text{Li}^+$ . It has been shown by

\* Corresponding author.

E-mail address: sb@nuclear.inin.mx (S. Bulbulian).

EPR [10] that defects induced in uranium soda phosphate glasses by external gamma irradiation may be caused by internal radioactive processes arising from the incorporated uranium.

Eschrich and Ochsenfeld [11] investigated the reprocessing of reactor fuels on an industrial scale using extraction chromatography. They performed some complementary studies related to the separation processes, such as radiation degradation of the stationary phase. They found that most of them were damaged at doses from 30 to 130 Mrad. These values were the starting point of our study.

Based on our previous experience with cobalt retention by zeolites, we have found it interesting to study the vitrification with temperature of those cobalt exchanged NaA and NaX zeolites [1–3] as well as the effect of gamma irradiation doses.

## 2. Experimental procedures

A and X synthetic powdered zeolites in the Na<sup>+</sup> form, with the following compositions: Na<sub>12</sub>Si<sub>12</sub>Al<sub>12</sub>O<sub>48</sub> · xH<sub>2</sub>O and Na<sub>86</sub>Si<sub>106</sub>Al<sub>86</sub>O<sub>384</sub> · xH<sub>2</sub>O, also alluded to, in this text, as AZ and XZ, respectively, were utilized to prepare cobalt exchanged zeolites. Other reagents were commercial analytical grade and used without further purification.

Each zeolite sample (20 g) initially in the sodium form was partially converted into the Co<sup>2+</sup> form by the addition of 400 ml of 0.05 N cobalt nitrate solution at room temperature. The mixtures were shaken for 3 h, and the solids were separated by centrifugation. They were then washed with deionized water. Cobalt uptake in the solids was determined by neutron activation analyses.

Thermal and irradiation effects were studied on the cobalt exchanged A and X zeolites (CoAZ and CoXZ). Thermally treated samples and  $\gamma$ -irradiated samples with a <sup>60</sup>Co gamma source, were characterized and tested for Co<sup>2+</sup> desorption when shaken with 1N NaCl solution for 2 h. Solids and liquids were separated by centrifugation, and the desorbed Co<sup>2+</sup> present in the NaCl solution was determined by neutron activation.

For neutron activation analyses, samples were irradiated in a Triga Mark III nuclear reactor for 15 minutes with an approximate neutron flux of 10<sup>13</sup> n/cm<sup>2</sup> s. The 1170 and 1330 photopeaks from <sup>60</sup>Co produced by the nuclear reaction <sup>59</sup>Co(*n*,  $\gamma$ )<sup>60</sup>Co were measured with a Ge/hyperpure solid-state detector coupled to a computerized 4096 channel pulse height analyzer.

CoAZ and CoXZ samples were heated at 400°C, 600°C, 700°C, 800°C, 900°C and 1000°C, and some samples were  $\gamma$ -irradiated in a <sup>60</sup>Co  $\gamma$ -beam at 100 or 600 Mrad. We chose to perform the irradiations at these doses because of the following considerations: the

amount of <sup>60</sup>Co that could load part of the cationic sites of zeolites A and X in 100 mg of zeolites A and X is around 0.1 mg of <sup>60</sup>Co with an activity of 2.5 × 10<sup>11</sup> Bq (6.8 × 10<sup>3</sup> mCi), which when in intimate contact with the zeolites, gives a dose rate of approximately 100 Mrad in one hour (89 Mrad/h) and 600 Mrad in a working day period (623 Mrad in 7 h).

Powder diffractograms were obtained with a Siemens D500 diffractometer coupled to a copper anode X-ray tube. The copper K<sub>z</sub><sup>-</sup> wavelength was selected with a diffracted beam monochromator. The conventional diffractograms were used to identify the compounds and to verify crystallinity, no smoothing function was used. The cell parameters were estimated by using internal standards: graphite for AZ and corundum for XZ zeolites. As the samples contained cobalt, the patterns presented a background due to the fluorescence of this metal with copper radiation. We chose, then, to determine the cell parameters with one peak, the one closest to the reference peak (corundum or graphite) to diminish the experimental error. This is highly recommended if the structure is cubic. Of course, in these measurements the peaks were scanned at a very slow speed ((1/8)°/min) and the curves smoothed to eliminate background contribution and to increase the accuracy on the determination of the 2 $\theta$  position of each peak (internal standard and sample).

The radial distribution functions were determined in samples treated at 800°C using a molybdenum anode X-ray tube to reach the high values of the angular parameter required for these studies. The intensities obtained by step scanning at 1/8°( $\Delta 2\theta$ ) were the input of the program Radiale [12].

IR spectra of samples in KBr pellets were recorded in the range 4000–350 cm<sup>-1</sup> by using a Nicolet Magna-IR spectrometer.

## 3. Results

### 3.1. Cobalt content

The neutron activation analysis of CoAZ and CoXZ samples showed that under the present experimental conditions, the cobalt content was 0.93 and 0.86 meq/g, respectively. These low cobalt retention values were selected in order to obtain low <sup>60</sup>Co<sup>2+</sup> charged zeolites, thereby, preventing cobalt desorption from the solid in the absence of external agents.

### 3.2. X-ray diffraction (compound identification)

X-ray diffraction showed that the crystalline structure of the AZ zeolite was stable up to 700°C. The sample treated at 800°C presented a large amount of carnegite (NaAlSiO<sub>4</sub>) although a low percentage of AZ

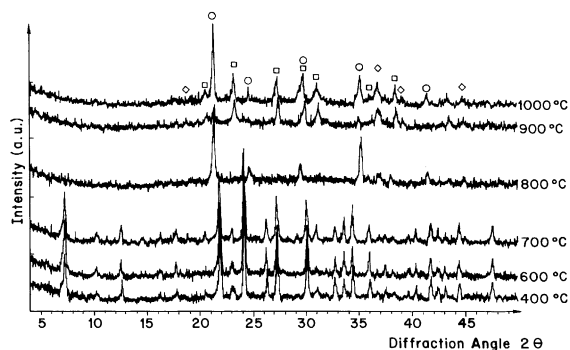


Fig. 1. X-ray diffraction patterns of thermally treated CoAZ zeolite. (□) nepheline, (○) carnegite, (◇) cobalt aluminate.

zeolite was still present. When the treatment temperature was 900°C, no zeolite peaks were observed; only carnegite and nepheline were found. The amount of nepheline was found to be higher in the 1000°C treated zeolites.

The faujasite structure was still present in XZ zeolites treated at 800°C. Samples treated at 900°C showed a broad background due to the presence of amorphous material and some intense peaks attributed to the formation of carnegite whereas, if treated at 1000°C, the sample was constituted by carnegite as well as nepheline.

Fig. 1 compares the X-ray diffraction patterns of the CoAZ zeolite thermally treated from 400°C to 1000°C. As expected, the 400°C treated sample reproduced the well-known diffractogram of zeolite A, the peaks are sharp and well defined, revealing that the crystalline structure was maintained. These features were also found in the 600°C and 700°C treated samples. Hence, CoAZ zeolite is thermally stable up to 700°C. Still, when the sample is treated at 800°C, the peaks present in the diffractogram correspond to carnegite and the broad background has to be attributed to an amorphous compound, most probably a glassy aluminosilicate. The samples treated at 900°C and 1000°C are constituted by carnegite, nepheline (which is a small pore zeolite and the most common of feldspathoids) and cobalt aluminate.

As treatment temperature was increased, the X-ray diffraction patterns (Fig. 2) showed that CoXZ samples maintained their crystallinity up to 700°C. Then, the sample turned out to be amorphous (900°C), i.e., a glassy aluminosilicate was formed which recrystallized at 1000°C as nepheline and small amounts of cobalt aluminate.

The previous sequences were reproduced by the irradiated samples. Therefore, the crystalline structure of CoAZ and CoXZ samples and the corresponding thermally treated samples were not altered by the  $\gamma$ -irradiation at 100 or 600 Mrad. Hence, in zeolites A and X,

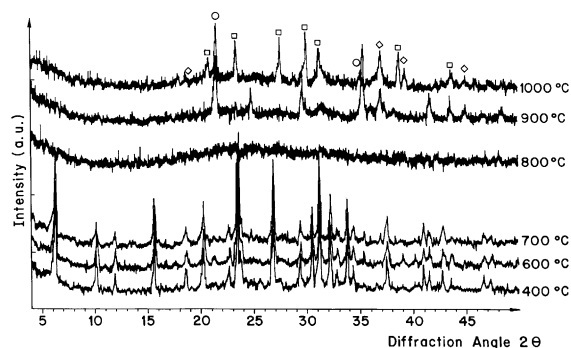


Fig. 2. X-ray diffraction patterns of thermally treated and  $\gamma$ -irradiated CoX zeolite. (□) nepheline, (○) carnegite, (◇) cobalt aluminate.

the amount of crystalline material, as a function of temperature, was not modified by the irradiation treatment.

### 3.3. X-ray diffraction (cell parameters)

To determine if there were any subtle modifications of the cell parameters, the  $2\theta$  location of the CoZA peak at  $2\theta$  ca.  $27.2^\circ$  was compared with the (002) graphite peak. In Fig. 3, the peak positions of the 400°C, 600°C and 700°C treated zeolites are compared. No differences were found in the non-irradiated zeolite A samples. As shown in Fig. 4 the peaks of the thermally treated CoXZ were all located in the same positions.

Fig. 5 shows that the peak (642) of the  $\gamma$ -irradiated (100 Mrad) AZ heated up to 700°C slightly shifted towards higher angles. The interplanar distances were, then, shorter due to a contraction of the crystalline lattice, which may be attributed to the combined action of irradiation and temperature. The same samples irradiated at 600 Mrad showed a clear expansion of the lattice 0.003 nm as the peaks were shifted (Fig. 6). In XZ irradiated samples at 100 Mrad (Fig. 7) the cell parameter

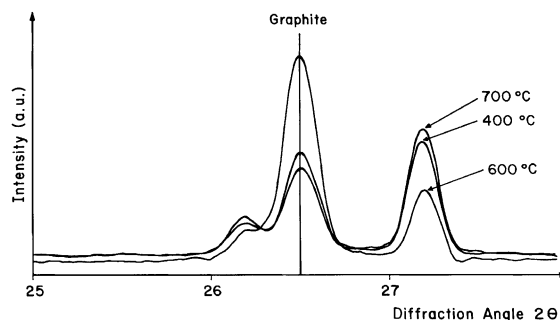


Fig. 3. Location of X-ray diffraction (642) peak of zeolite A compared with the (002) peak of graphite, non-irradiated samples.

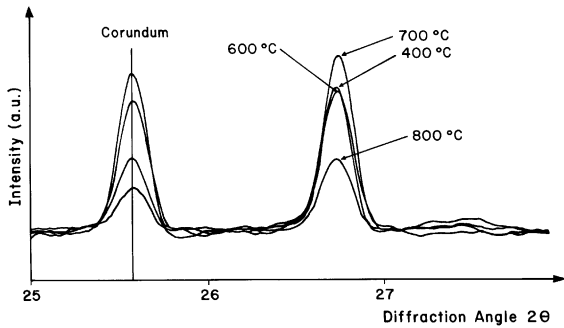


Fig. 4. Location of X-ray diffraction (642/246) peak of zeolite X compared with the (012) peak of corundum, non-irradiated samples.

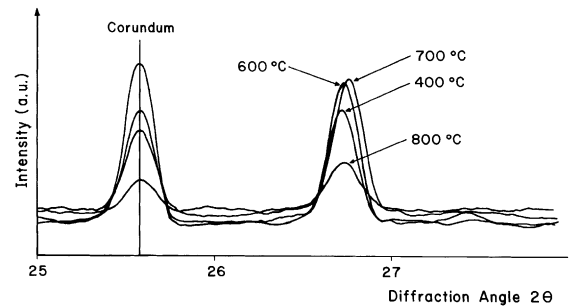


Fig. 7. Location of X-ray diffraction (642/246) peak of zeolite X compared with the (012) peak of corundum, irradiated samples (100 Mrad).

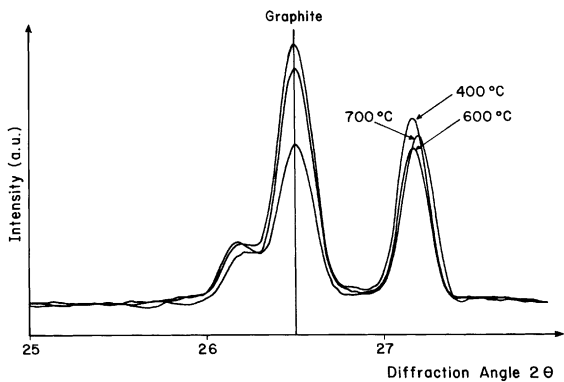


Fig. 5. Location of X-ray diffraction (642) peak of zeolite A compared with the (002) peak of graphite, irradiated samples (100 Mrad).

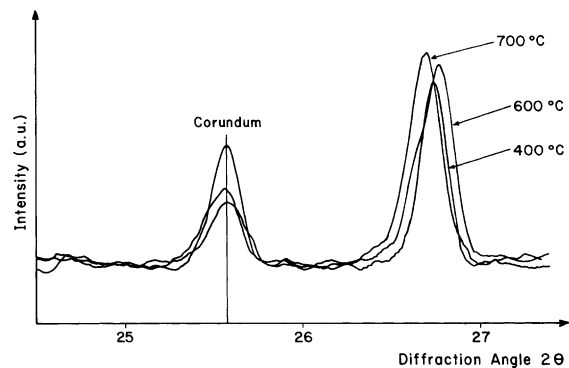


Fig. 8. Location of X-ray diffraction (642/246) peak of zeolite X compared with the (012) peak of corundum, irradiated samples (600 Mrad).

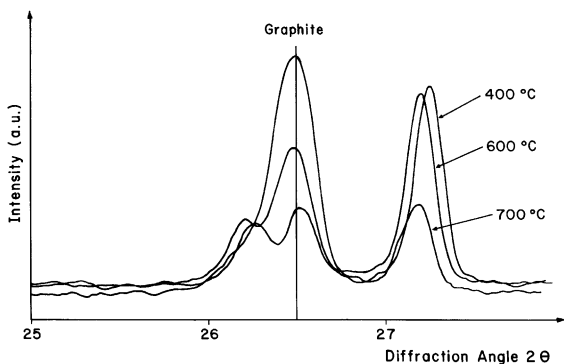


Fig. 6. Location of X-ray diffraction (642) peak of zeolite A compared with the (002) peak of graphite, irradiated samples (600 Mrad).

was also modified 0.003 nm. A variation of 0.006 nm was observed for 600 Mrad treatment in samples heated at 800 °C (Fig. 8). Again, the combined action of temperature and irradiation (100 or 600 Mrad) contracted

the zeolite network most probably by the elimination of structural water molecules.

### 3.4. X-ray diffraction (radial distribution functions)

Fig. 9 compares the radial distribution functions of the non-irradiated, irradiated at 100 and 600 Mrad Co-zeolite A. No significant modifications are observed in the position or shape of the peaks for radial distances shorter than 0.5 nm. The first neighbor distances are then the same in the three samples. For second neighbor distances, i.e., distances larger than 0.5 nm, the order is higher in irradiated samples than in the calcined zeolites. Fig. 10 presents the radial distribution functions of the Co-zeolite X treated at 800, non-irradiated, irradiated at 100 or 600 Mrad. In this last sample the curve is better defined for radial distances higher than 0.5 nm. Hence if the first neighbor distances are the same in the three samples the irradiation at 600 Mrad provides more defined second neighbor distances, i.e., a higher long-range order. Note that in these functions no distance can be

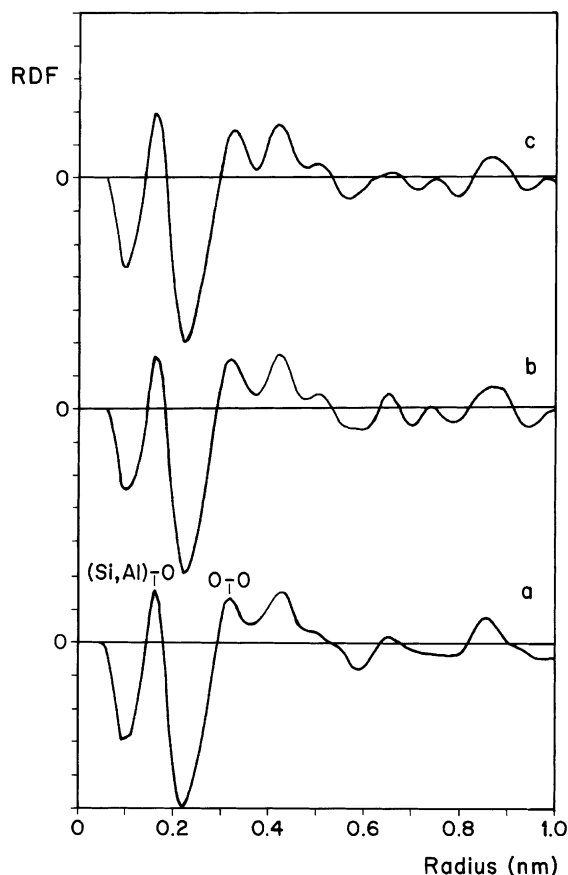


Fig. 9. Radial distribution function of the zeolite A (a) treated at 800°C; (b) treated at 800°C and irradiated at 100 Mrad and (c) treated at 800°C and irradiated at 600 Mrad.

attributed to Co–O bonds. The content of cobalt is very low and the corresponding small peak should appear between radius values of 0.199 and 0.213 nm. This peak cannot be resolved as the (Si, Al)–O is very close and masks it.

### 3.5. IR spectroscopy

Figs. 11 and 12 show the IR spectra of AZ and XZ zeolite samples, respectively. The columns correspond to the zeolites heated at various temperatures. Our interest was mainly focused on the bands from 500 to 600  $\text{cm}^{-1}$  and from 320 to 420  $\text{cm}^{-1}$ .

In zeolite IR spectra a band in the 500–600 region is related to the presence of the double ring in the framework structure and is observed in all zeolite structures that contain the double 4- and the double 6-ring [13]. The frequencies in the 300–420  $\text{cm}^{-1}$  portion of the spectrum are related to the pore opening in the zeolites. It appears to be fairly observable depending upon the type of zeolite structure [13].

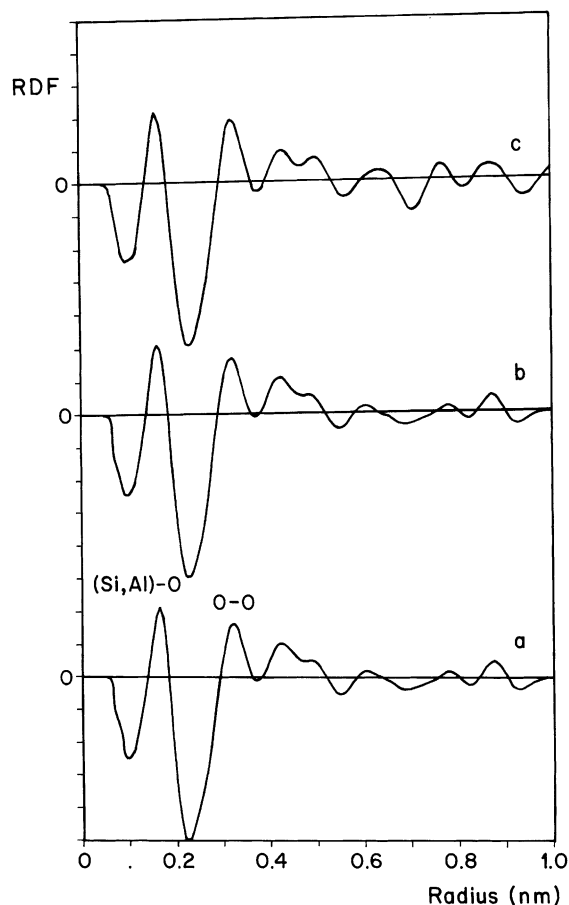


Fig. 10. Radial distribution functions of the zeolite X (a) treated at 800°C; (b) treated at 800°C and irradiated at 100 Mrad and (c) treated at 800°C and irradiated at 600 Mrad.

The IR spectra of AZ zeolite showed its stability up to 700°C. Fig. 11(a) shows the vibration frequency at 546  $\text{cm}^{-1}$  related to the presence of the double ring of AZ zeolite. The frequency at 372  $\text{cm}^{-1}$  assigned to the pore-opening of the external linkage disappeared in the samples that were heated from 800°C to 1000°C (Figs. 11(b)–(d)). It is worth noting that at 1000°C (Fig. 11(d)) new vibration frequencies at 551 and 513  $\text{cm}^{-1}$  appeared, and they are assigned to the presence of the double rings of one or two different zeolites.

The corresponding IR spectra of XZ zeolite (Figs. 12(a)–(d)) show that the stability of XZ zeolites under thermal treatment is lower than that of AZ zeolite. The vibration frequencies present at 1073 and 750  $\text{cm}^{-1}$  in zeolite XZ (Fig. 12(a)) were assigned, respectively, to the asymmetric and symmetric stretch associated with external linkages [13]. Vibration frequency at 570  $\text{cm}^{-1}$  can be related to the presence of a double ring, and finally the frequency at 364  $\text{cm}^{-1}$  can be assigned to the pore opening of the external linkages [13]. These frequencies

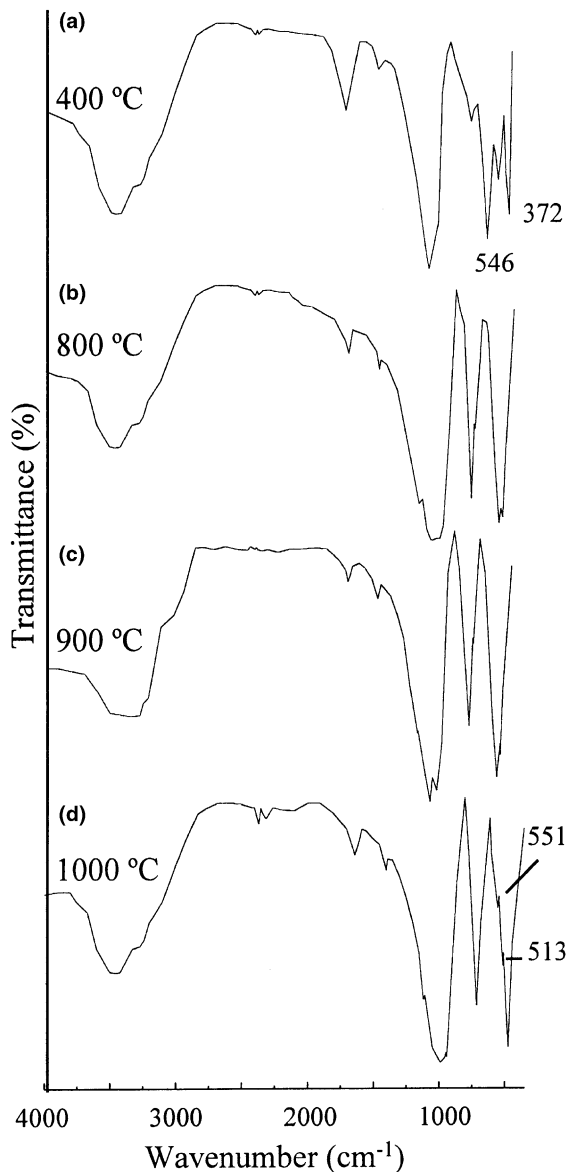


Fig. 11. IR spectra of AZ zeolite samples heated at 400°C (a), 800°C (b), 900°C (c) and 1000°C (d).

lost intensity at 800°C (Fig. 12(b)) and disappeared in the samples heated at 900°C and 1000°C (Figs. 12(c) and (d)). However at 1000°C (Fig. 12(d)) the vibration of the double ring of a new zeolite, probably nepheline, appeared at 517  $\text{cm}^{-1}$ .

IR absorption bands were also studied in CoAZ and CoXZ zeolite samples. The IR absorption which might be attributed to Na–O in the original and the Co–O bondings in the exchanged zeolite structures were not observed since these characteristic frequencies generally occur below 350  $\text{cm}^{-1}$ , beyond the spectral region studied. However, some differences were found between

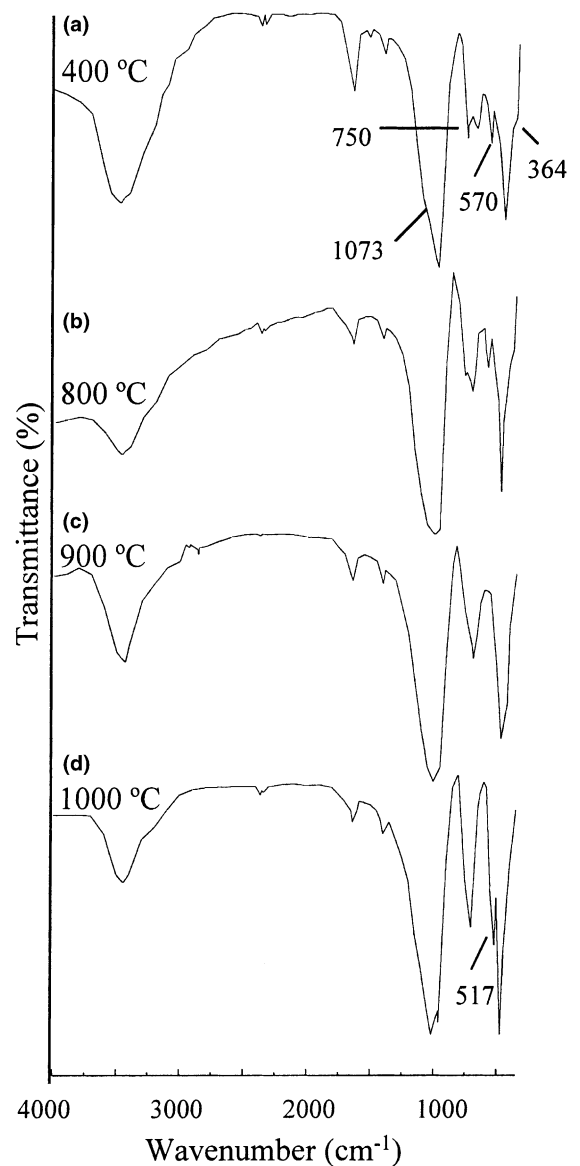


Fig. 12. IR spectra of XZ zeolite samples heated at 400°C (a), 800°C (b), 900°C (c) and 1000°C (d).

the Co exchanged zeolites and the original A zeolite. Fig. 13(a) shows the IR absorption bands of CoAZ zeolite heated at 1000°C. The bands attributed to the double rings of a zeolite found in the AZ sample heated at the same temperature (Fig. 11(d)) are missing in the CoAZ sample (Fig. 13(a)), but when heated at 1000°C and irradiated at 600 Mrad a low intensity band at 511  $\text{cm}^{-1}$  was observed (Fig. 13(b)) which is comparable to the 513  $\text{cm}^{-1}$  absorption found for AZ sample heated at 1000°C.

On the other hand IR spectra of  $\gamma$ -irradiated CoXZ zeolites at 600 Mrad showed additional destruction of the crystalline structure; moreover already at 800°C the

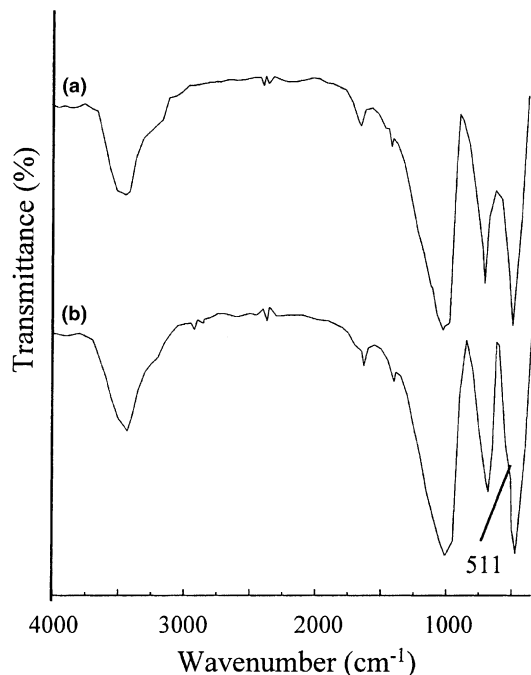


Fig. 13. IR spectra of CoAZ zeolite samples heated at 1000°C, (a) non-irradiated, (b) irradiated at 600 Mrad.

IR bands attributed to the double ring of the XZ sample are missing (Fig. 14(a)). However CoXZ heated at 900°C and 1000°C showed a band at 515 cm<sup>-1</sup> comparable to that (517 cm<sup>-1</sup>) of sample XZ heated at 1000°C (Fig. 12(d)).

These results show that thermal treatment and  $\gamma$ -irradiation, mainly at 600 Mrad, modify moderately the CoAZ zeolites and more intensively CoXZ zeolite. This conclusion is complementary to the X-ray diffraction results. IR spectra seem to be much more sensitive to local structural modifications.

### 3.6. Co<sup>2+</sup> desorption from the solids when in contact with 1N NaCl solution

The cobalt desorption from the samples, when in contact with 1N NaCl solution, was studied. The cobalt desorption curves as determined by neutron activation are shown in Figs. 15(a) and (b).

Although XRD and IR studies showed some damage in CoAZ sample irradiated at 600 Mrad. However, cobalt desorption analyses were not sensitive and did not show any radiation effects on CoAZ samples  $\gamma$ -irradiated at either 100 or 600 Mrad. Their behavior were indeed similar to that observed in the non-irradiated samples. Fig. 15(a) shows that small amounts of cobalt were desorbed (around 20%) from CoAZ heated at 400°C. This value decreased continuously for higher

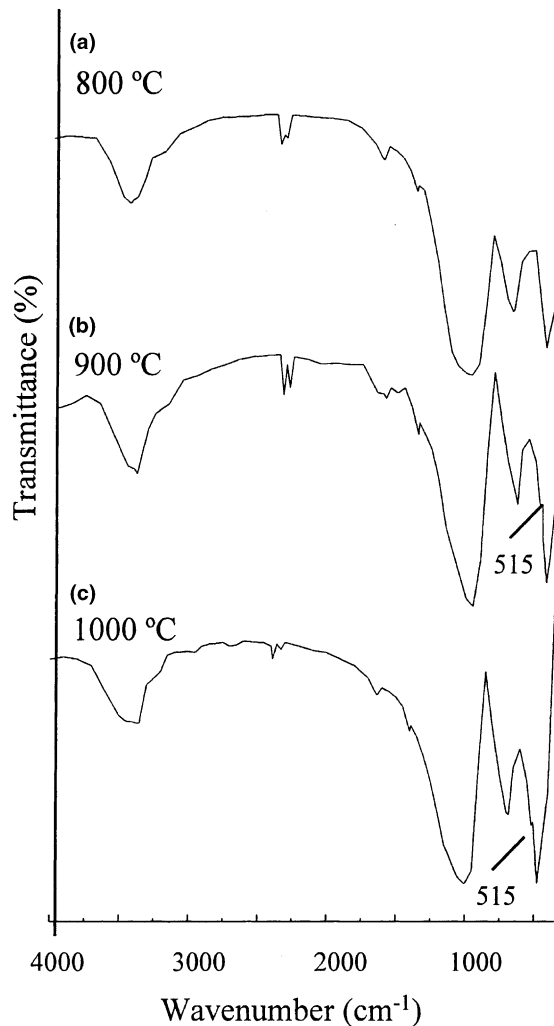


Fig. 14. IR spectra of CoXZ zeolite samples heated at 800°C (a), 900°C (b) and 1000°C (c) and irradiated at 600 Mrad.

heating temperatures. At 800°C and higher temperatures, when the CoAZ zeolite was fully vitrified, cobalt was trapped in the amorphous solid and no cobalt desorption was detected.

In contrast, in CoXZ a clear radiation effect was observed. Cobalt desorption analyses on CoXZ showed that  $\gamma$ -irradiation altered considerably the structure of the zeolite (Fig. 15(b)). This effect was not noticeable at 400°C; however, already at 600°C and higher temperatures it was clear. Cobalt desorption on CoXZ sample heated at 400°C either non-irradiated or irradiated at 100 Mrad was found to be about 55%, but this percentage decreased considerably for higher heating temperatures. Cobalt desorption decreased from 45% for the non-irradiated zeolite heated at 700°C to 40% for the CoXZ  $\gamma$ -irradiated at 100 Mrad and to 32% for zeolite  $\gamma$ -irradiated at 600 Mrad. In the case of samples heated at

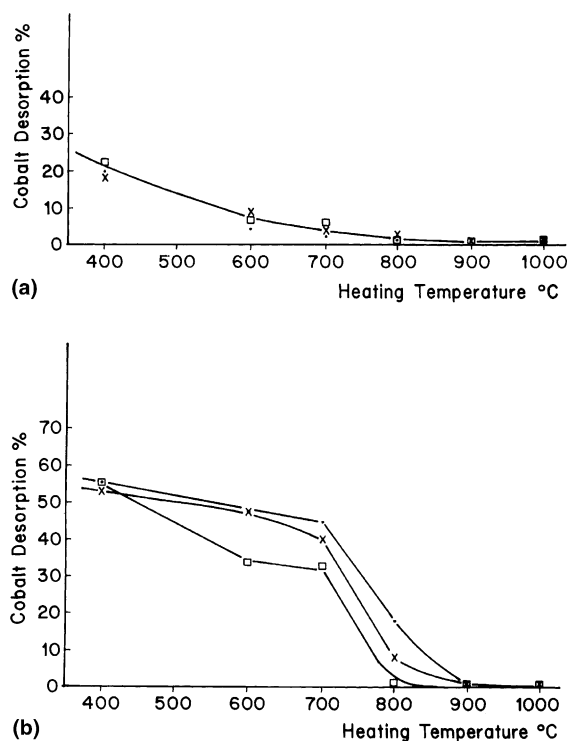


Fig. 15. Cobalt desorption with 1N NaCl solution (a) from CoAZ zeolite and (b) from CoXZ zeolite.

800°C, cobalt desorption was of 18% for the non-irradiated CoXZ zeolite, 8% for the sample irradiated at 100 Mrad and less than 0.2% for the CoXZ sample irradiated at 600 Mrad.

#### 4. Discussion

Both, X-ray diffraction and Infrared spectroscopy were in agreement about the characterization of the zeolites. These techniques are complementary and provide a full and adequate characterization of the samples.

With temperature the zeolite structure collapsed and cobalt was trapped in the amorphous lattice of the vitrified materials. Cobalt did not diffuse out from the vitrified solid when it was left in contact with a sodium chloride solution. Furthermore, nepheline (crystallized in the sample heated at 1000°C) did not contain cobalt as the balancing cation, as no cobalt was desorbed. Therefore, the Co–O bonds were more stable in the glasses than in the zeolites. The thermal treatment produced similar effects in both zeolites.

Irradiation at high doses produced the formation of composite materials different from those obtained with thermal treatment. In this sense, the variations of cell parameters and IR spectra were clear. Hence, the

differences in cobalt desorption behavior found in zeolite X can be correlated with those structural variations induced by irradiation. With irradiation, most probably, the initial cobalt exchanged zeolite suffered a photoinduced redistribution of chemical bonds. Irradiation with gamma rays produced point defects and these defects favored diffusion. The easier the diffusion, the easier the vitrification. Therefore, as cobalt was retained into the vitrified lattice, irradiation enhanced cobalt retention.

Zeolite X was more sensitive to irradiation effects than zeolite A; zeolite X crystalline structure is less dense and hence less stable. Therefore, irradiation penetrated deeper in zeolite X. Last but not least, the Si/Al ratio of the glassy material present in those composite materials after thermal and irradiation treatments was different and was not a determining parameter in the cobalt retention in this amorphous structure.

#### 5. Conclusions

The main conclusions which emerge from this study are the following:

1. Radioactive cobalt was trapped firmly in type A and X zeolites when the zeolites were vitrified at temperatures higher than 700°C and 800°C, respectively.
2. In zeolite X, the irradiation effects arising from the incorporation of radioactive material, simulated by external  $\gamma$ -radiation, showed that  $\gamma$ -radiation promoted vitrification of cobalt exchanged zeolites. It can, therefore, enhance the cobalt retention.
3. With a thermal treatment at temperatures up to 1000°C, a zeolite (nepheline) crystallized selectively. Cobalt remained, indeed, trapped in the glassy material and the balancing cation of the zeolite was not cobalt.

#### Acknowledgements

The assistance of H. Pfeiffer and the technical work of M. Villa-Tomas, E. Morales, A. Anastacio Montes and V.H. Lara are gratefully acknowledged and appreciated.

#### References

- [1] P. Bosch, I. García, M. Solache, S. Bulbulian, *Sep. Sci. Technol.* 30 (17) (1995) 3403.
- [2] I. García, M. Solache-Ríos, P. Bosch, S. Bulbulian, *Langmuir* 12 (1996) 4474.
- [3] I. Nava, I. García-Sosa, M. Solache-Ríos, *Radioanal. Nucl. Chem. Articles* 191 (1) (1995) 83.
- [4] A.C. Buechele, I.S. Muller, I.L. Pegg, C. Kim, E. Yashenko, *Ceram. Trans.* 61 (1995) 203.



- [5] M. Földesová, P. Lukác, J. Majling, V. Tomková, *J. Radioanal. Nucl. Chem. Lett.* 212 (4) (1996) 293.
- [6] L. Thamzil, Waste treatment immobilization technologies involving inorganic sorbents, Final Report of a Coordinated Research Program, 1992–1996. International Atomic Energy Agency, Vienna, Austria, 1997.
- [7] Th. Gerber, B. Himmel, H. Lorenz, D. Stachel, *Cryst. Res. Technol.* 23 (10/11) (1988) 1293.
- [8] A.J. Leadbetter, A.C. Wright, *J. Non-Cryst. Solids* 7 (1972) 37.
- [9] A. Marotta, A. Aronne, P. Pernice, M. Catauro, *Mater. Chem. Phys.* 42 (1995) 247.
- [10] V. Simon, I. Ardelean, O. Cozar, S. Simon, *J. Mater. Sci. Lett.* 15 (1996) 784.
- [11] H. Eschrich, W. Ochsenfeld, *Sep. Sci. Technol.* 15 (4) (1980) 697.
- [12] M. Magini, A. Cabrini, *J. Appl. Crystallogr.* 5 (1972) 14.
- [13] D.W. Breck, in: *Zeolite Molecular Sieves*, Wiley, New York, 1974.